Sensitivity of Surface Complexation Modeling to the Surface Site Density Parameter

SABINE GOLDBERG

United States Department of Agriculture, Agricultural Research Service, U.S. Salinity Laboratory, 4500 Glenwood Drive, Riverside, California 92501

Received October 8, 1990; accepted January 23, 1991

Previous research has shown that adsorption of many inorganic anions on soil mineral surfaces can be described equally well by chemical surface complexation models using either inner- or outer-sphere surface complexes. At the same time, goodness of fit of these models to adsorption data has been used to distinguish between inner- and outer-sphere adsorption mechanisms. In this study the ability of chemical surface complexation models to describe anion adsorption on goethite using both inner- and outer-sphere surface complexes was evaluated and found to be sensitively dependent on the value of the surface site density. Application of a goodness of fit criterion leads to the choice of an inner-sphere adsorption mechanism for small surface site densities and an outer-sphere adsorption mechanism for large values of this parameter. Experimentally determined values of surface site density vary by an order of magnitude depending upon the method used. It is suggested that uncertainty in the value of the surface site density parameter currently invalidates use of surface complexation models to predict anion adsorption mechanisms on soil mineral surfaces. © 1991 Academic Press, Inc.

INTRODUCTION

Surface complexation models, such as the triple-layer model (1–3) and the constant capacitance model (4), are chemical models that use an equilibrium approach to describe the formation of complexes at the oxide–solution interface. Unlike empirical models, such as the Langmuir and Freundlich adsorption isotherm equations, chemical models explicitly define surface species, chemical reactions, equilibrium constant expressions, and surface activity coefficient expressions. Additional advantages of surface complexation models are inclusion of mass and charge balance equations and consideration of the charge on both the adsorbate and the adsorbent.

To provide a molecular description of adsorption processes, surface complexation models assume a detailed structure of the interfacial region (5). Surface species are defined as outer-sphere complexes, containing at least one water molecule between the adsorbate ion and the surface functional group, or as inner-sphere complexes, containing no water molecules between the adsorbate ion and the surface functional group. In the original triple-layer model, all adsorbate ions are assumed to form outer-sphere surface complexes (2, 3). The constant capacitance model assumes inner-sphere configurations for all surface complexes (4). The modified triple-layer model allows the user to choose between inner- and outer-sphere surface complexes for all adsorbed surface complexes (6).

Although surface complexation models are very successful at describing experimental data over a wide range of conditions, they cannot, at present, be used to describe uniquely the structure of surface complexes (7). Good quantitative descriptions of calcium, magnesium, cadmium, copper, and lead adsorption isotherm experimental data can be obtained with either inner-sphere (8–10) or outer-sphere (2, 11) surface complexes. For describing phosphate, selenite, arsenate, salycilate,

0021-9797/91 $3.00
Copyright © 1991 by Academic Press, Inc.
All rights of reproduction in any form reserved.

and phthalate adsorption, use of either inner-sphere (12–16) or outer-sphere (17–19) complexes provides good fits to the experimental data.

Currently, to provide a correct chemical representation, independent experimental evidence for a particular adsorption mechanism and surface structure must be used when choosing the appropriate chemical surface complexation model. Independent spectroscopic evidence has been cited to validate use of inner-sphere surface complexes for phosphate (12), arsenate (15), selenite, and selenate (20) adsorption. Pressure-jump kinetic experiments have been linked with surface complexation modeling to establish adsorption mechanisms for phosphate (17), chromate (21), lead (6), molybdate (22), sulfate (23), selenite, and selenate (24). However, since results from surface complexation modeling of an equilibrium study are necessary to analyze the kinetic data, this approach is not independent. Mikami *et al.* (17), using pressure-jump kinetics with surface complexation modeling, concluded that phosphate ions adsorb on aluminum oxide as outer-sphere surface complexes. This conclusion directly contradicts much experimental evidence supporting an inner-sphere adsorption mechanism for phosphate (25).

The surface site density is an important parameter in surface complexation models. Its value has been either determined experimentally by tritium exchange (2, 3), potentiometric titration (10, 11, 16), or maximum anion adsorption (12, 14, 15) or optimized to fit the data (20). Experimental determinations of surface site density for goethite range from 4 sites/nm^2 for potentiometric titration to 6–7 sites/nm^2 for fluoride adsorption to 17 sites/nm^2 for tritium exchange (26). Crystallographic calculations of reactive surface hydroxyl groups on goethite yield approximately 3 sites/nm^2 (5). Sensitivity analyses showed that surface complexation models were relatively insensitive to surface site density values for amorphous hydrous ferric oxide in the range of 3 to 12 sites/nm^2 (20) and for a soil in the range of 1.25 to 2.5 sites/nm^2 (27).

In this study, surface complexation models will be evaluated for their ability to fit anion adsorption data on goethite using various experimental values of surface site density. Goethite was chosen as the adsorbent because its surface site density and anion adsorption behavior have been extensively characterized. Both inner-sphere and outer-sphere adsorption mechanisms will be tested and evaluated as to their sensitivity to the surface site density parameter.

DATA AND METHODS

The constant capacitance model (4) and the triple-layer model, modified to allow both inner- and outer-sphere adsorption mechanisms (6), were the surface complexation models used in the study. Chemical assumptions, chemical reactions, intrinsic conditional equilibrium constants for protonation–dissociation and background electrolyte complex formation, mass balance and charge balance equations for the constant capacitance, and the triple-layer models are discussed in detail in Sposito (5). For both models a generalized reaction for the formation of inner-sphere anion surface complexes is

$$\equiv\mathrm{FeOH}_{(s)} + \mathrm{H}_y A_{(aq)} = \equiv\mathrm{FeH}_{(y-1-x)}A^{-x}_{(s)} + H_2O + x\mathrm{H}^+_{(aq)}. \quad [1]$$

For the modified triple-layer model a generalized reaction for the formation of outer-sphere anion surface complexes is

$$\equiv\mathrm{FeOH}_{(s)} + \mathrm{H}_y A_{(aq)} = \equiv\mathrm{FeOH}^+_2 - \mathrm{H}_{(y-z)}A^{-z}_{(s)} + (z-1)\mathrm{H}^+_{(aq)}, \quad [2]$$

where y is the number of protons present in the undissociated form of the acid, A is the completely dissociated form of the acid, $-x$ is the charge on the inner-sphere anion surface complex ($x = 0$, 1, or 2), $-z$ is the charge on the anion portion of the outer-sphere anion surface complex ($z = 1$, 2, or 3), and ≡FeOH

represents 1 mol of reactive surface hydroxyls bound to an Fe^{3+} ion in the goethite mineral.

The above reactions are described by the following intrinsic conditional equilibrium constant expressions for inner-sphere anion surface complex formation,

$$K_A^i(\text{int}) = \frac{[\equiv\text{FeH}_{(y-1-x)}A^{-x}][\text{H}^+]^x}{[\equiv\text{FeOH}][\text{H}_yA]} \times \exp(-xF\psi_o/RT), \quad [3]$$

and outer-sphere anion surface complex formation,

$$K_A^i(\text{int}) = \frac{[\text{FeOH}_2^+ - \text{H}_{(y-z)}A^{-z}][\text{H}^+]^{(z-1)}}{[\equiv\text{FeOH}][\text{H}_yA]} \times \exp[F(\psi_o - z\psi_\beta)/RT]. \quad [4]$$

where $i = x + 1 = z$, F (C mol_c^{-1}) is the Faraday constant, R is the molar gas constant, T is the absolute temperature, ψ_o (V) is the potential at the o plane, ψ_β (V) is the potential at the β plane, and square brackets represent concentrations (mol liter^{-1}). Analogous to solution equilibria, the number of anion surface complexes included in the model is equal to the number of dissociations undergone by the acid. Therefore, the number of surface complexation reactions is three for phosphate and arsenate, two for selenite, selenate, sulfate, molybdate, and silicate, and one for borate.

The computer program FITEQL (28) was used to obtain values of the intrinsic surface complexation constants, log K_A^i(int). FITEQL contains both the constant capacitance model and the triple-layer model and uses a nonlinear least-squares optimization technique to fit equilibrium constants to experimental adsorption data. Anion surface complexation constants that were present in insignificant amounts ($<10^{-15}$) were dropped from the FITEQL optimizations. This procedure was necessary because it is sometimes impossible to obtain convergence of the FITEQL program for species present at very small concentrations.

For the constant capacitance modeling, anion adsorption data were obtained from Hingston (29) for phosphate, selenite, silicate, and arsenate and from Goldberg and Glaubig (30) for borate. FITEQL optimizations of these adsorption data had been carried out previously using maximum anion adsorption values for the surface site density, $[\text{SOH}]_T$ (14, 15, 30). Additional FITEQL optimizations were carried out in this study using the surface site density value of 7 sites/nm^2 optimized by Hayes *et al.* (20) for selenium adsorption and using $[\text{SOH}]_T$ obtained from the crystallographic calculations of Sposito (5), 0.305 nm^2 per A-type surface hydroxyl group.

For the triple-layer modeling, anion adsorption data were obtained from Hayes *et al.* (20) and Zhang and Sparks (24) for selenite and selenate, from Zhang and Sparks (22) for molybdate, and from Zhang and Sparks (23) for sulfate. FITEQL optimizations of these adsorption data had been carried out by the authors. Hayes *et al.* (20) had used a surface site density value of 7 sites/nm^2 based on best fit. Zhang and Sparks (22–24) had used a surface site density value of 6.4 sites/nm^2 obtained from potentiometric titration data. Additional FITEQL optimizations were carried out in this study using the authors' values of intrinsic conditional equilibrium constants for protonation–dissociation and background electrolyte surface complex formation and capacitance density parameters. Surface site density values used in this study were obtained from the authors, from crystallographic calculations by Sposito (5), and from maximum anion adsorption by Hingston (31).

RESULTS AND DISCUSSION

Numerical values obtained for the intrinsic surface complexation constants using the constant capacitance model are provided in Table I. All anions investigated are considered to adsorb specifically, that is, to form inner-sphere surface complexes (15, 32), since such an anion surface configuration is assumed in the constant capacitance model. In Table I, surface site density, $[\text{SOH}]_T$, increases from

TABLE I

Numerical Values of Intrinsic Surface Complexation Constants Using the Constant Capacitance Model

Solid	$[SOH]_T$ from maximum adsorption				$[SOH]_T$ = 0.305 nm² per *A*-type hydroxyl				$[SOH]_T$ = 7 sites/nm²			
	$\log K_A^1$	$\log K_A^2$	$\log K_A^3$	SOS/DF	$\log K_A^1$	$\log K_A^2$	$\log K_A^3$	SOS/DF	$\log K_A^1$	$\log K_A^2$	$\log K_A^3$	SOS/DF
Goethite A												
Arsenate	10.10	5.80	−0.63	0.7	6.57	2.60	−2.53	1.9			−7.40	47
Phosphate	10.84	6.78	0.52	0.6	6.73	3.08	−1.91	2.8			−7.12	102
Goethite B												
Phosphate	10.43	6.25	0.17	0.06	7.20	3.67	−0.66	1.3		Overflow		
Silicate	3.82	−4.27		0.1		Overflow				Singular		
Goethite C												
Arsenate	10.87	6.52	0.29	2.0	8.18	4.50	−0.35	4.6		Overflow		
Phosphate	10.49	6.27	0.17	0.5	7.31	3.37	−1.29	3.5			−7.07	52
Selenite	10.02	5.36		0.8	7.74	3.75		3.4		−0.41		95
Goethite E												
Phosphate	11.80	9.02	3.16	0.03	7.63	5.24	0.32	0.2			−4.73	26
Selenite	11.10	5.80		27	7.61	3.41		155		Overflow		
Silicate	4.48	−3.43		0.4	2.18	−3.80		1.7		Overflow		
Goethite												
Borate	5.12			3.2	1.85			8.9	1.47			11

Note. Experimental data for goethites A, B, C, and E from Hingston (29). Experimental data for goethite from Goldberg and Glaubig (30). Maximum adsorption values, $[SOH]_T$, are given in Goldberg (15) for goethite A; in Goldberg (14) for goethites B, C, and E; and in Goldberg and Glaubig (30) for goethite. The sum of squares over the degrees of freedom, SOS/DF, is an indicator of goodness of fit.

left to right. It can be seen that for all anions, without exception, the values of $\log K_A^i(\text{int})$ decrease and the values of SOS/DF, a goodness-of-fit criterion, increase with increasing surface site density. Since the smallest values of SOS/DF indicate the best fits, the best fits of the constant capacitance model are obtained for the smallest values of $[SOH]_T$. Additionally, as $[SOH]_T$ values increase, convergence of the FITEQL program becomes more difficult; overflow and singularity problems are two types of convergence problems.

The fit of the constant capacitance model to borate adsorption on goethite as a function of pH is shown in Fig. 1 for three different values of surface site density. The borate surface complexation constant $\log K_B(\text{int})$ was the only parameter optimized by the FITEQL program. Under these conditions, only the smallest value of $[SOH]_T$, obtained from maximum adsorption, provides a reasonable fit to the borate adsorption data.

Table II provides numerical values obtained for the intrinsic surface complexation constants using both the inner-sphere and the

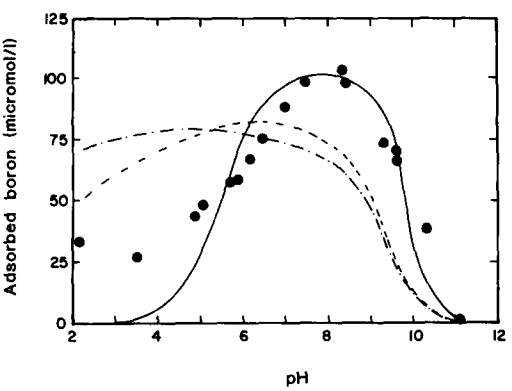

FIG. 1. Borate adsorption on goethite. Experimental data (●) from Goldberg and Glaubig (30). Constant capacitance model results are represented by (—) for $[SOH]_T$ = maximum adsorption, by (---) for $[SOH]_T$ = 0.305 nm² per hydroxyl, and by (-·-·) for $[SOH]_T$ = 7 sites/nm².

TABLE II

Numerical Values of Intrinsic Surface Complexation Constants Using the Triple-Layer Model

Solid	$\log K_A^1$	$\log K_A^2$	SOS/DF	$\log K_A^1$	$\log K_A^2$	SOS/DF	$\log K_A^1$	$\log K_A^2$	SOS/DF
	Experimental data from Hayes *et al.* (20)								
	$[SOH]_T$ = 0.91 nm^2 per SeO_4 ion			$[SOH]_T$ = 0.305 nm^2 per *A*-type hydroxyl			$[SOH]_T$ = 7 sites/nm^2		
Selenate									
1.0 *M*									
Inner-sphere		5.12	25		3.23	210		2.56	245
Outer-sphere	13.90	8.19	11	No convergence			13.58	7.45	15
0.1 *M*									
Inner-sphere		6.52	299		5.35	517		4.66	591
Outer-sphere	14.35	8.10	11	14.24	7.71	13	14.18	7.44	15
0.01 *M*									
Inner-sphere		7.42	327		6.46	460		5.83	537
Outer-sphere	13.99	8.22	73	14.13	7.54	78	14.14	7.11	77
0.001 *M*									
Inner-sphere		7.67	481		6.79	489		6.19	523
Outer-sphere		8.04	331		7.28	270		6.83	218
	$[SOH]_T$ = 0.537 nm^2 per SeO_3 ion			$[SOH]_T$ = 0.305 nm^2 per *A*-type hydroxyl			$[SOH]_T$ = 7 sites/nm^2		
Selenite									
1.0 *M*									
Inner-sphere		5.74	1700		5.56	1752		5.24	176
Outer-sphere	12.03	2.51	427	12.22		321	11.73		284
0.1 *M*									
Inner-sphere		5.13	998		4.97	1192		4.70	1435
Outer-sphere	11.99	3.40	259	11.88	2.71	272	11.71	1.55	212
0.005 *M*									
Inner-sphere		5.53	8.4		5.39	22		5.17	58
Outer-sphere	13.88	3.71	15	13.56	3.00	12	13.08	0.007	8.2
	Experimental data from Zhang and Sparks (24)								
	$[SOH]_T$ = 0.91 nm^2 per SeO_4 ion			$[SOH]_T$ = 0.305 nm^2 per *A*-type hydroxyl			$[SOH]_T$ = 6.4 sites/nm^2		
Selenate									
Inner-sphere	9.92	6.53	15		3.56	129		2.51	237
Outer-sphere	11.26	9.02	5.2	10.24	8.26	8.2	9.89	7.64	7.6
	$[SOH]_T$ = 0.537 nm^2 per SeO_3 ion			$[SOH]_T$ = 0.305 nm^2 per *A*-type hydroxyl			$[SOH]_T$ = 6.4 sites/nm^2		
Selenite									
Inner-sphere	11.01	7.96	6.6	8.23	6.15	20		3.33	528
Outer-sphere	13.02	9.03	4.8	No convergence			10.90	8.52	18
	Experimental data from Zhang and Sparks (23)								
	$[SOH]_T$ = 0.90 nm^2 per SeO_4 ion			$[SOH]_T$ = 0.305 nm^2 per *A*-type hydroxyl			$[SOH]_T$ = 6.4 sites/nm^2		
Sulfate									
Inner-sphere	11.97	6.70	17		3.83	97		0.91	692
Outer-sphere	14.44	12.69	12	11.00	10.92	2.9	10.43	10.10	2.4

TABLE II—*Continued*

Solid	log K_A^1	log K_A^2	SOS/DF	log K_A^1	log K_A^2	SOS/DF	log K_A^1	log K_A^2	SOS/DF
	Experimental data from Zhang and Sparks (22)								
	$[SOH]_T$ = 0.337 nm^2 per MoO_4 ion			$[SOH]_T$ = 0.305 nm^2 per *A*-type hydroxyl			$[SOH]_T$ = 6.4 sites/nm^2		
Molybdate									
0.1 *M*									
Inner-sphere	4.77	−0.04	15	4.32	−0.63	13		−2.69	12
Outer-sphere	7.71	5.25	7.1	7.65	5.21	8.5	7.30	4.71	29
0.05 *M*									
Inner-sphere	4.79	−0.09	20	4.26	−0.99	16		−2.60	9.7
Outer-sphere	7.73	4.83	5.8	7.67	4.79	6.4	7.34	4.44	16
0.01 *M*									
Inner-sphere	4.38	−0.006	11	3.95	−0.58	12		−2.94	21
Outer-sphere	7.35	4.38	2.5	7.29	4.35	2.6	6.98	4.05	3.1

Note. The sum of squares over the degrees of freedom, SOS/DF, is an indicator of goodness of fit.

outer-sphere surface complexes and the triple-layer model. As in Table I, surface site density, $[SOH]_T$, increases from left to right. For inner-sphere complex formation of most anions, the values of log K_A^i(int) decrease and the values of SOS/DF increase with increasing surface site density. When describing inner-sphere complex formation, the triple-layer model, as well as the constant capacitance model, provides the best fits for the smallest values of $[SOH]_T$. For outer-sphere complex formation of most anions, values of log K_A^i(int) and SOS/DF exhibit a much smaller dependence on the magnitude of surface site density.

Figure 2 shows the fit of the triple-layer model to selenite adsorption on goethite as a function of pH for three different values of surface site density using both inner-sphere (Fig. 2a) and outer-sphere (Fig. 2b) surface complex configurations. The fit for both types of surface complexes and all surface site densities is good. For the inner-sphere surface complex the best fit is obtained for the smallest value of surface site density, while for the outer-sphere surface complex the largest value of $[SOH]_T$ provides the best fit. Selenite adsorption on goethite has been reported to occur through the formation of inner-sphere complexes using direct spectroscopic measurements (33). Application of goodness-of-fit criteria would have lead to the choice of an outer-sphere adsorption mechanism for the largest surface site density value, in direct contradiction with the direct spectroscopic evidence. Only for the smallest surface site density would goodness-of-fit criteria have chosen an adsorption mechanism that is in agreement with the spectroscopic results.

The fit of the triple-layer model to selenate adsorption on goethite as a function of pH is indicated in Fig. 3 for various values of $[SOH]_T$ using both inner-sphere (Fig. 3a) and outer-sphere (Fig. 3b) surface complexes. For inner-sphere adsorption, an acceptable fit is obtained only for the smallest value of surface site density. For outer-sphere adsorption, the fit for all values of $[SOH]_T$ is uniformly good and almost independent of the value of $[SOH]_T$. Selenate adsorption on goethite has been reported to occur via outer-sphere complex formation using direct spectroscopic measurements (33). In the case of selenate, application of goodness-of-fit criteria leads to the choice of an outer-sphere adsorption mechanism for all surface site densities, in agreement with the spectroscopic evidence.

Figure 4 shows the fit of the triple-layer model to sulfate adsorption on goethite as a

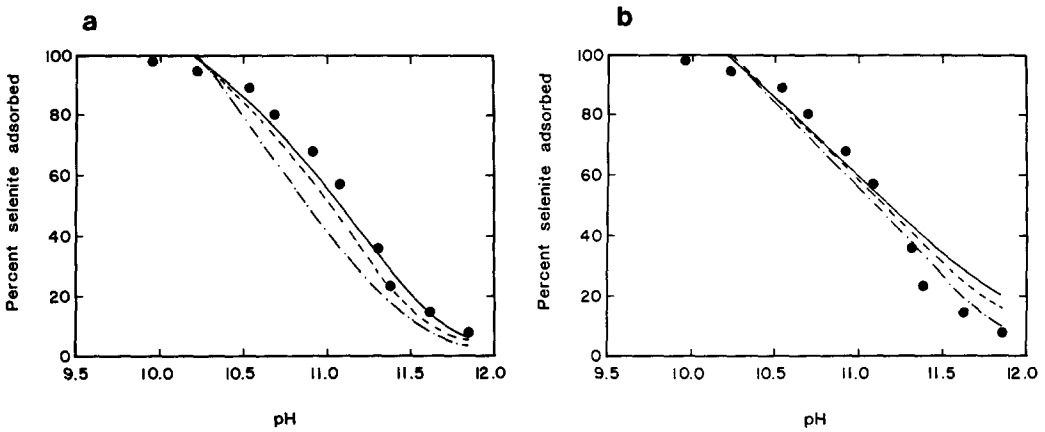

FIG. 2. Selenite adsorption on goethite: (a) inner-sphere mechanism, (b) outer-sphere mechanism. Experimental data (●) from Hayes *et al.* (20). Triple-layer model results are represented by (—) for $[SOH]_T$ = maximum adsorption, from Hingston (31), by (---) for $[SOH]_T$ = 0.305 nm^2 per hydroxyl, and by (-·-·) for $[SOH]_T$ = 7 sites/nm^2.

function of pH and surface site density using both inner-sphere (Fig. 4a) and outer-sphere (Fig. 4b) surface complexes. For the inner-sphere surface complex the fit is extremely poor except for the smallest value of surface site density. For the outer-sphere surface complex the fit, as for selenate (Fig. 3b), is good for all values of $[SOH]_T$ and shows little dependence on $[SOH]_T$. Sulfate adsorption behavior is "intermediate" in that it exhibits certain characteristics representative of inner-sphere and some representative of outer-sphere surface complexes (5). The exact adsorption mechanism for sulfate has not yet been identified with spectroscopic methods.

The fit of the triple-layer model to molybdate adsorption on goethite as a function of pH and $[SOH]_T$ is shown in Fig. 5 using both inner-sphere (Fig. 5a) and outer-sphere (Fig. 5b) surface complex configurations. For inner-

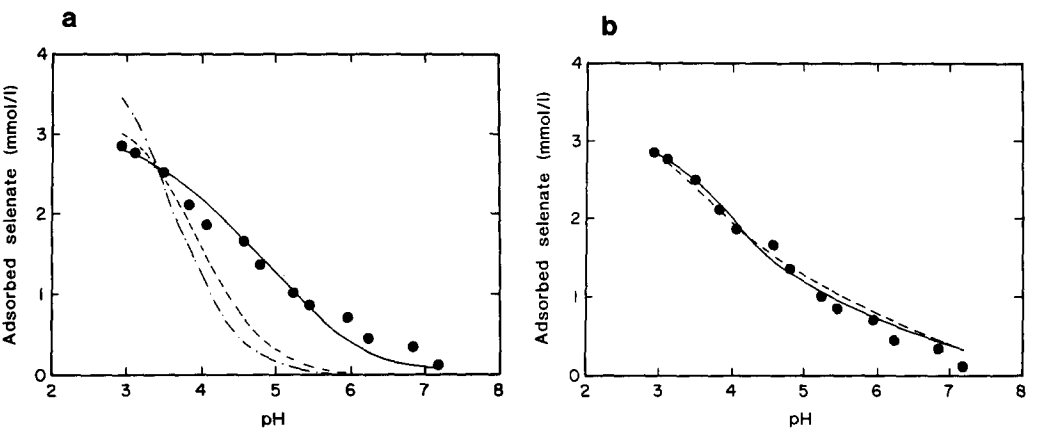

FIG. 3. Selenate adsorption on goethite: (a) inner-sphere mechanism, (b) outer-sphere mechanism. Experimental data (●) from Zhang and Sparks (24). Triple-layer model results are represented by (—) for $[SOH]_T$ = maximum adsorption, from Hingston (31), by (---) for $[SOH]_T$ = 0.305 nm^2 per hydroxyl, and by (-·-·) for $[SOH]_T$ = 6.4 sites/nm^2.

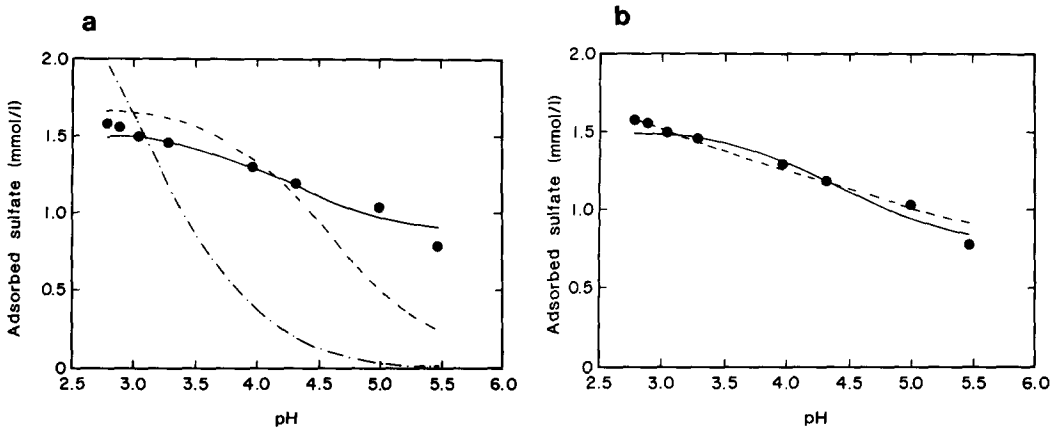

FIG. 4. Sulfate adsorption on goethite: (a) inner-sphere mechanism, (b) outer-sphere mechanism. Experimental data (●) from Zhang and Sparks (23). Triple-layer model results are represented by (—) for $[SOH]_T$ = maximum adsorption, from Hingston (31), by (---) for $[SOH]_T$ = 0.305 nm^2 per hydroxyl, and by (-·-·) for $[SOH]_T$ = 6.4 sites/nm^2.

sphere adsorption, the best fit is obtained for the smallest value of surface site density, although all fits are poor. For outer-sphere adsorption, as for selenate (Fig. 3b) and sulfate (Fig. 4b), the fit is good for all $[SOH]_T$ values and virtually independent of $[SOH]_T$. Molybdate adsorption on goethite and gibbsite occurs via a ligand exchange mechanism forming inner-sphere complexes (34). Application of goodness-of-fit criteria would have lead to the choice of an outer-sphere adsorption mechanism for all surface site densities, in direct contradiction with the indirect experimental results of Hingston *et al.* (34).

CONCLUSIONS

The ability of the constant capacitance model and the triple-layer model to describe anion adsorption on goethite using both inner-

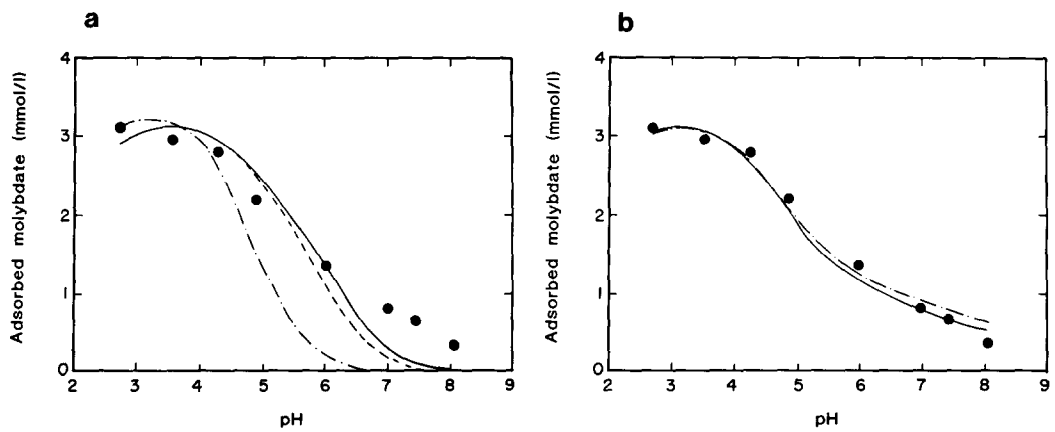

FIG. 5. Molybdate adsorption on goethite: (a) inner-sphere mechanism, (b) outer-sphere mechanism. Experimental data (●) from Zhang and Sparks (22). Triple-layer model results are represented by (—) for $[SOH]_T$ = maximum adsorption, from Hingston (31), by (---) for $[SOH]_T$ = 0.305 nm^2 per hydroxyl, and by (-·-·) for $[SOH]_T$ = 6.4 sites/nm^2.

and outer-sphere surface complexes was evaluated and found to be sensitively dependent on the value of the surface site density. Application of a goodness-of-fit criterion leads to the choice of an inner-sphere adsorption mechanism for small surface site densities and an outer-sphere adsorption mechanism for large values of $[SOH]_T$. Experimental determinations of $[SOH]_T$ vary by an order of magnitude depending on the type of method used. Uncertainty in the value of $[SOH]_T$ currently invalidates use of surface complexation models to distinguish anion adsorption mechanisms on soil mineral surfaces. Independent experimental evidence is required to choose the appropriate adsorption mechanism for surface complexation modeling. Further research is needed to determine the most appropriate experimental measurement of surface site density for describing anion adsorption. Because of the sensitivity to this parameter, agreement among researchers on a preferred experimental methodology would be most useful for the continued development of surface complexation modeling.

REFERENCES

1. Davis, J. A., James, R. O., and Leckie, J. O., *J. Colloid Interface Sci.* **63,** 480 (1978).
2. Davis, J. A., and Leckie, J. O., *J. Colloid Interface Sci.* **67,** 90 (1978).
3. Davis, J. A., and Leckie, J. O., *J. Colloid Interface Sci.* **74,** 32 (1980).
4. Stumm, W., Kummert, R., and Sigg, L., *Croat. Chem. Acta* **53,** 291 (1980).
5. Sposito, G., "The Surface Chemistry of Soils," p. 234. Oxford Univ. Press, Oxford, 1984.
6. Hayes, K. F., and Leckie, J. O., *ACS Symp. Ser.* **323,** 114 (1986).
7. Westall, J., and Hohl, H., *Adv. Colloid Interface Sci.* **12,** 265 (1980).
8. Huang, C.-P., and Stumm, W., *J. Colloid Interface Sci.* **43,** 409 (1973).
9. Schindler, P. W., Fuerst, B., Dick, R., and Wolf, P. U., *J. Colloid Interface Sci.* **55,** 469 (1976).
10. Hohl, H., and Stumm, W., *J. Colloid Interface Sci.* **55,** 281 (1976).
11. Balistrieri, L. S., and Murray, J. W., *Am. J. Sci.* **281,** 788 (1981).
12. Goldberg, S., and Sposito, G., *Soil Sci. Soc. Am. J.* **48,** 772 (1984).
13. Hawke, D., Carpenter, P. D., and Hunter, K. A., *Environ. Sci. Technol.* **23,** 187 (1989).
14. Goldberg, S., *Soil Sci. Soc. Am. J.* **49,** 851 (1985).
15. Goldberg, S., *Soil Sci. Soc. Am. J.* **50,** 1154 (1986).
16. Kummert, R., and Stumm, W., *J. Colloid Interface Sci.* **75,** 373 (1980).
17. Mikami, N., Sasaki, M., Hachiya, K., Astumian, R. D., Ikeda, T., and Yasunaga, T., *J. Phys. Chem.* **87,** 1454 (1983).
18. Benjamin, M. M., and Bloom, N. S., *in* "Adsorption from Aqueous Solution" (P. H. Tewari, Ed.), p. 41. Plenum, New York, 1981.
19. Balistrieri, L. S., and Murray, J. W., *Geochim. Cosmochim. Acta* **51,** 1151 (1987).
20. Hayes, K. F., Papelis, C., and Leckie, J. O., *J. Colloid Interface Sci.* **125,** 717 (1988).
21. Mikami, N., Sasaki, M., Kikuchi, T., and Yasunaga, T., *J. Phys. Chem.* **87,** 5245 (1983).
22. Zhang, P. C., and Sparks, D. L., *Soil Sci. Soc. Am. J.* **53,** 1028 (1989).
23. Zhang, P. C., and Sparks, D. L., *Soil Sci. Soc. Am. J.* **54,** 1266 (1990).
24. Zhang, P. C., and Sparks, D. L., *Environ. Sci. Technol.* **24,** 1848 (1990).
25. Goldberg, S., and Sposito, G., *Commun. Soil Sci. Plant Anal.* **16,** 801 (1985).
26. Sigg, L. M., "Die Wechselwirkung von Anionen und Schwachen Saeuren mit αFeOOH (Goethit) in Waessriger Loesung," p. 141. Ph.D. Thesis. Swiss Federal Institute of Technology, Zurich, 1979.
27. Goldberg, S., and Sposito, G., *Soil Sci. Soc. Am. J.* **48,** 779 (1984).
28. Westall, J. C., "FITEQL: A Computer Program for Determination of Equilibrium Constants from Experimental Data," p. 101. Report 82-01. Department of Chemistry, Oregon State University, Corvallis, 1982.
29. Hingston, F. J., "Specific Adsorption of Anions on Goethite and Gibbsite," p. 479. Ph.D. Thesis. University of Western Australia, Nedlands, 1970.
30. Goldberg, S., and Glaubig, R. A., *Soil Sci. Soc. Am. J.* **49,** 1374 (1985).
31. Hingston, F. J., *in* "Adsorption of Inorganics at Solid–Liquid Interfaces" (M. A. Anderson and A. J. Rubin, Eds.), p. 51. Ann Arbor Science, Ann Arbor, MI, 1980.
32. Mott, C. J. B., *in* "The Chemistry of Soil Processes" (D. J. Greenland and M. H. B. Hayes, Eds.), p. 179. Wiley, Chichester, UK, 1981.
33. Hayes, K. F., Roe, A. L., Brown, G. E., Hodgson, K. O., Leckie, J. O., and Parks, G. A., *Science* **238,** 783 (1987).
34. Hingston, F. J., Posner, A. M., and Quirk, J. P., *J. Soil Sci.* **23,** 177 (1972).